

Liquid-Phase Broadband Cavity-Enhanced Absorption Spectroscopy Measurements in a 2 mm Cuvette

MEEZ ISLAM,* L. NITIN SEETOHUL, and ZULFIQUR ALI

School of Science and Technology, University of Teesside, Borough Road, Middlesbrough TS1 3BA

A novel implementation of broadband cavity enhanced absorption spectroscopy (BBCEAS) has been used to perform sensitive visible wavelength measurements on liquid-phase solutions in a 2 mm cuvette placed at normal incidence to the cavity mirrors. The overall experimental methodology was simple, low cost, and similar to conventional ultraviolet-visible absorption spectroscopy. The cavity was formed by two concave high reflectivity mirrors. Three mirror sets with nominal reflectivities (R) of $R = 0.99$, 0.9945 , and 0.999 were used. The light source consisted of a high intensity red, green, blue, or white LED. The detector was a compact charge-coupled device (CCD) spectrograph. Measurements were made on the representative analytes, Ho^{3+} , and the dyes brilliant blue-R, sudan black, and coumarin 334 in appropriate solvents. Cavity enhancement factors (CEF) of up to 104 passes for the high reflectivity mirrors were obtained. The number of passes was limited by relatively high scattering and absorption losses in the cavity, of $\sim 1 \times 10^{-2}$ per pass. Measurements over a wide wavelength range (420–670 nm) were also obtained in a single experiment with the white LED and the $R = 0.99$ mirror set for Ho^{3+} and sudan black. The sensitivity of the experimental setup could be determined by calculating the minimum detectable change in the absorption coefficient α_{min} . The values ranged from 5.1×10^{-5} to $1.2 \times 10^{-3} \text{ cm}^{-1}$. The limit of detection (LOD) for the strong absorber brilliant blue-R was 620 pM. A linear dynamic range of measurements of concentration over about two orders of magnitude was demonstrated. The overall sensitivity of the experimental setup compared very favorably with previous generally more experimentally complex and expensive liquid-phase cavity studies. Possible improvements to the technique and its applicability as an analytical tool are discussed.

Index Headings: Broadband cavity-enhanced absorption spectroscopy; BBCEAS; Liquids; Absorption detection; Light emitting diode; LED.

INTRODUCTION

Absorption spectroscopy is one of the most widely used and useful analytical techniques. This stems from all atomic and molecular species displaying an absorption spectrum somewhere in the electromagnetic spectrum. Furthermore, absorption spectroscopy can be used in a quantitative manner through the application of the Beer–Lambert law, which can be expressed as

$$\log_{10} \frac{I_0}{I} = \epsilon Cl \quad (1)$$

where I_0 is the intensity of light in the absence of a sample, I is the transmitted intensity, ϵ is the wavelength-dependent molar extinction coefficient, C is the concentration of the sample, and l is the path length of light through the sample. When compared to competing but less widely applicable analytical techniques such as fluorescence based measurements, the sensitivity of conventional absorption spectroscopy is considered to be poorer because weak absorptions require the

detection of small changes in intensity against a large background signal. However, over the last two decades optical cavity based methods have been used to increase the sensitivity of absorption spectroscopy. These methods rely on light being confined between two high reflectivity mirrors, which results in the base path length being increased by many orders of magnitude in the gas phase. The first implementation of this technique was cavity ring down spectroscopy (CRDS), which was proposed by O’Keefe and Deacon in 1988.¹ Typically, light from a pulsed laser or a continuous wave (cw) laser with a suitable interruption method is introduced into the cavity through the back of one of the mirrors. In CRDS, the $1/e$ decay time, known as the ring-down time, of a pulse of laser light confined between the mirrors is measured in the presence and absence of a sample and related to the absorption coefficient α (where $\alpha = 2.303\epsilon C$) at a particular wavelength of the sample in the optical cavity. The wavelength can be scanned in most cases to record an absorption spectrum. The detection of the light exiting the cavity requires fast response detectors and associated equipment capable of measuring on the nanosecond to microsecond timescale. This, along with the expense of pulsed laser sources and interruption methods for cw lasers makes most implementations of CRDS relatively expensive.

In 1998 Engeln et al.² and O’Keefe³ published details of a simpler variation of CRDS, respectively named cavity-enhanced absorption spectroscopy (CEAS) and integrated cavity output spectroscopy (ICOS). In essence, both implementations are equivalent and the term CEAS will be used for the remainder of the paper. In CEAS, a cw laser light source is used, but unlike cw CRDS, the time-integrated output from the cavity is measured in the absence and presence of a sample rather than the ring-down time. This reduces the experimental complexity because the data analysis does not require determination of ring-down times; also, slower response detectors can be used, which reduces the cost of the detection side of the experimental scheme. However, the absorption coefficient now cannot be measured directly because the mirror reflectivity is not obtained from the measurement. Instead, the mirror reflectivity must be separately determined by CRDS or the mirrors must be calibrated with a reference compound of known concentration and extinction coefficient in the cavity, which absorbs over the wavelength range of the measurement. A further disadvantage is that conventional CEAS measurements are generally less sensitive than comparable CRDS measurements.⁴

Further experimental simplification of CEAS techniques is possible through the replacement of the cw laser light source. Recently, simpler and cheaper light sources have been proposed.^{5–7} These light sources include broadband light sources such as arc lamps or high intensity light emitting diodes (LEDs), and the technique has been termed broadband CEAS (BBCEAS). The use of a broadband light source

Received 26 January 2007; accepted 19 March 2007.

* Author to whom correspondence should be sent. E-mail: m.islam@tees.ac.uk.

typically requires the use of a multiplex detector such as a charge-coupled device (CCD) spectrograph or a Fourier transform instrument. This provides the advantage of multiplex spectroscopy because the entire absorption spectrum is recorded in a single measurement, while conventional CEAS requires scanning of the cw laser light source across a wavelength range to obtain the absorption spectrum. A potential disadvantage exists in that the wavelength resolution for the absorption spectrum is determined by the resolution of the multiplex detector and in most cases is significantly lower than that of conventional CEAS where the wavelength resolution is determined by the linewidth of the cw laser source. Thus, for high-resolution gas-phase measurements BBCEAS would not appear to be suitable.

Optical cavity based studies are now a relatively mature experimental field, as evidenced by the number of reviews of CRDS and CEAS.^{8–14} Recent trends in the field appear to be heading in disparate directions. New variants on CEAS such as noise-immune cavity-enhanced optical heterodyne spectroscopy (NICE-OHMS)¹⁵ and optical feedback CEAS¹⁶ have increased the sensitivity of the technique at the expense of cost and experimental simplicity. Other techniques, such as BBCEAS, fiber loop ring-down spectroscopy (FLRDS),¹⁷ and phase shift fiber loop ring-down spectroscopy (PS-FLRDS),¹⁸ have sacrificed ultimate sensitivity for experimental simplicity, low cost, and applicability to other phases.

Cavity ringdown spectroscopy and CEAS have principally been used for the detection of gases having narrow absorption features. More recently there has been increasing interest in applying these techniques to the analysis of liquids, in which most absorption features are relatively broad (>10 nm line width). Also, in practice, the number of species available for study in the liquid-phase is far greater than those in the gas phase. Consequently, the application of CRDS and CEAS to the liquid phase makes the techniques much more widely applicable analytical tools. Xu et al.¹⁹ provided the first demonstration of liquid-phase CRDS using a quartz cuvette filled with fractional mixtures of benzene in hexane and the detection of the fifth overtone CH stretch in benzene at ~607 nm. The cuvette was placed at Brewster's angle to minimize reflection losses from *p*-polarized laser light. A small number of other liquid-phase studies have been reported to date. These are mainly CRDS based and involved either a cuvette in a cavity^{20,21} or a cell in which the mirrors are in direct contact with the liquid sample.^{22,23} A few studies have applied liquid-phase CRDS to high-performance liquid chromatography (HPLC) systems.^{24–27} Currently, only two studies using CEAS for liquid-phase measurements have been reported. Fielder et al.²⁸ made cuvette based measurements at normal angles of incidence using BBCEAS in a modified conventional double beam ultraviolet (UV)-visible spectrometer. The absorption studied was the fifth overtone of the CH stretch in benzene at ~607 nm. Recently, McGarvey et al.²⁹ reported CEAS measurements on the biomolecule bacteriochlorophyll *a* made at 783 nm using a Titanium:Sapphire laser system locked to a cavity resonance and high reflectivity mirrors in direct contact with the liquid sample. One drawback of liquid-phase studies is that the losses due to scattering and or absorption by the solvent and the cuvette windows can be significant and can reduce the number of passes compared to gas-phase measurements. However, through the use of high reflectivity mirrors, careful choice of solvents, and reduction of scatter from cuvette

surfaces, greater than 1000 passes have been demonstrated for liquid-phase CRDS studies^{22–27} and also recently for CEAS measurements.²⁹

At first glance, BBCEAS would appear to be a less than ideal method for the study of liquids. The inability to measure the absorption coefficient directly as well as the significantly lower wavelength resolution would appear to be disadvantages. However, for liquids most absorption features are relatively broad and easily resolvable with a standard spectrograph. Although the absorption coefficient cannot be measured directly, a calibration with a reference compound can be performed relatively simply. Advantages of using BBCEAS for liquid-phase measurements include experimental simplicity and lower cost. The light source is a lamp or high intensity LED rather than a laser, and also, expensive fast detection equipment is not needed. Multiplex detectors such as CCD spectrographs are now available at low cost. The use of multiplex detection means that in principle several species can be detected simultaneously. There is also a similarity in the methodology for making an absorption measurement to conventional UV-visible spectroscopy. Another advantage over liquid-phase CRDS occurs when using short sample path lengths. For CRDS measurements, short sample path lengths, associated with using cuvettes, would typically require picosecond laser sources and nanosecond timescale detection or an increase of the path length between the cavity mirrors to lengthen the ringdown time. For BBCEAS, because a ringdown time is not measured, the experimental difficulty does not increase for a short sample path length.

The aim of this study was to investigate an experimentally simple, low-cost implementation of liquid-phase BBCEAS in a 2 mm quartz cuvette and study a number of representative analytes over a range of wavelengths in the visible part of the spectrum. This work further makes a comparison of the sensitivity of the technique with previous more experimentally complex and expensive liquid-phase cavity-based studies.

EXPERIMENTAL

The experimental setup for liquid-phase BBCEAS consisted of three major components: the broadband light source, the cavity, and the multiplex detector.

Broadband Light Source. The first BBCEAS study carried out by Fielder et al.⁵ used a custom built Xenon arc lamp as the light source. This had the advantage of high spectral radiance ($18 \text{ W cm}^{-2} \text{ nm}^{-1} \text{ sr}^{-1}$ at 400 nm), but similar commercial lamps are relatively expensive. Recently, high intensity LEDs have become available. Although significantly less powerful than a Xenon arc lamp, these are available at a range of visible wavelengths with power outputs greater than 200 mW, low power consumption, long lifetimes, and very low cost. It was decided to use these as the broadband light source for liquid-phase experiments, although during the course of this study Ball et al.⁶ published their study on gas-phase BBCEAS also using high intensity LEDs. The LEDs used for this study were from the 'O star' range of Luxeon 1 W devices (Lumileds, San Jose, CA). These were supplied with an integral collimator that reduced the divergence of the output to ~10 degrees. The central emission wavelength of the red, green, and blue LEDs was 630, 535, and 455 nm, respectively, while the bandwidths were approximately 20, 35, and 20 nm, respectively. A white LED covering the range 450–700 nm was also used for some of the measurements.

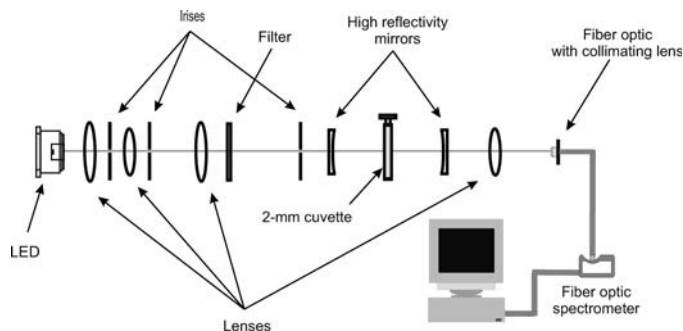


FIG. 1. A schematic of the experimental setup for the liquid-phase BBCEAS measurements.

Cavity. The cavity was formed by two high reflectivity concave mirrors separated by 5 cm. A quartz cuvette with a 2 mm path (Optiglass Ltd, UK) was mounted on a rotation stage (Thorlabs, UK) and placed in the cavity at 0 degrees angle of incidence. Although previous studies have placed optical components in the cavity at Brewster's angle in order to minimize loss due to reflection,^{19,21,24} Fielder et al.²⁸ showed that a similar local minimum in the reflectivity also exists at 0 degrees angle of incidence. Even though there is a ~4% reflection loss per surface at 0 degrees, in a cavity this reflected light is in theory recycled into the cavity. This local minimum varies more sharply than the minimum at Brewster's angle but allows easier alignment of the optical component and also is present for unpolarized light, unlike the Brewster's angle minimum, which requires *p*-polarized light.

The choice of high reflectivity mirrors for BBCEAS experiments was not straightforward. Initially, the requirement was for high reflectivity mirrors ($R > 0.999$) with a bandwidth of 300 nm covering the range 400–700 nm. Although such dielectric mirrors can be fabricated, the large bandwidth requires multistack designs that result in significant ripples in the reflectivity curve as a function of wavelength. At certain points the reflectivity can vary by more than a factor of 10. This introduces problems when the output from the cavity is detected with a CCD spectrograph because the variation of intensity as a function of wavelength can result in saturation at certain pixels and low counts at others. As a result of this information it was decided to instead obtain "standard" design high reflectivity mirrors, which have a bandwidth of ~100 nm and a relatively flat variation of reflectivity with wavelength. Three mirror sets nominally of blue, green, and red wavelengths were obtained (Laseroptik, Germany), covering the range 400–700 nm with $R > 0.999$, a diameter of 25 mm, and a radius of curvature of ~1500 mm. Initial experiments, however, revealed that aside from the red LED and red mirror set, insufficient light intensity after the cavity could be detected with the CCD spectrograph once the cuvette was inserted into the cavity. Consequently, a set of lower reflectivity mirrors ($R = 0.99$) was obtained (Layertec, Germany). These had an effective range from 420 to 670 nm, and although there are ripples in the reflectivity curve as a function of wavelength at this lower reflectivity, their effect on the variation of the intensity of the cavity light as a function of wavelength is significantly smaller and does not limit detection with a CCD spectrograph. In addition to the high reflectivity and low reflectivity mirror sets, an intermediate reflectivity mirror set could be created by combining the mirror sets ($R = (R_1R_2)^{1/2} =$

0.9945). These mirror reflectivities assume the minimum manufacturer's specification and were not verified by independent CRDS measurements.

Charge-Coupled Device Spectrograph. The light exiting the cavity was detected by a compact CCD spectrograph (Avantes AVS2000). This low-cost device consisted of a factory-sealed unit that contained an *f*/4, 42 mm focal length asymmetrically crossed Czerny–Turner design spectrograph bench. The detector was an uncooled 2048 element linear silicon CCD array (Sony ILX511). A 600 lines/mm grating with a blaze wavelength of 400 nm provided a spectral range of 200 to 850 nm and in combination with a 25 μm entrance slit resulted in a spectral resolution of 1.5 nm. Light was coupled into the spectrometer through an SMA905 fiber-optic connector. The device was powered through a USB port, which also allowed data transfer. The software package Avasoft (Avantes, The Netherlands) was used to control the spectrometer and record spectra. The lack of thermoelectric cooling of the CCD sensor resulted in relatively high levels of dark noise and restricted the use of long integration time. The maximum integration time that could be used with acceptable noise was three seconds. This is far lower than the integration times that can be used with scientific-grade thermoelectrically cooled CCD arrays, albeit these devices are significantly more expensive.

Experimental Optimization and Choice of Analytes and Solvents. A schematic of the experimental setup is shown in Fig. 1. The output from the LED was partially collimated by the integrated optic to a divergence angle of ~10 degrees; however, this was insufficient for alignment through the cavity. A series of lenses and irises were used to further collimate the beam. This resulted in only a small fraction of the initial output from the LED reaching the first mirror of the cavity. At best, about 1% of the LED output remained after collimation, and this remains a disadvantage of using astigmatic light sources such as LEDs, which are inherently difficult to collimate sufficiently. By contrast, laser light sources are generally well collimated and most of the output can be used. Although all the O star Luxeon LEDs were quoted to have the same divergence, within the experimental setup it was found that the red LED was better collimated than the blue, green, or white LEDs. This resulted in experiments with the red LED and two $R = 0.999$ mirrors being possible, while this was not possible with the other LEDs for which insufficient light reached the detector with this mirror set.

The quartz cuvette was mounted on a rotation stage and placed equidistant between the two cavity mirrors. The typical alignment procedure for the cavity involved, first, alignment of the cavity without the cuvette by maximizing the output of the LED reaching the spectrograph at a given integration time by iterative adjustment of the front and back cavity mirrors. The cuvette was then placed in the cavity with a blank solvent solution. This resulted in a large decrease in the intensity reaching the spectrograph due to interface losses at the cuvette windows and the solvent. The integration time was increased appropriately to ensure that the signal from the LED was significantly above the dark noise level but not high enough to saturate the detector. Typical integration times for the three mirror sets with the red LED were ~10 ms for the $R = 0.99$ set, ~150 ms for the $R = 0.9945$ set, and ~2 s for the $R = 0.999$ set. As mentioned earlier, the use of the green and blue LEDs resulted in lower light intensities reaching the detector, and

thus longer integration times for the $R = 0.99$ and 0.9945 mirror sets had to be used, while insufficient intensity was present for use with the $R = 0.999$ mirror set. Likewise, the white LED produced even lower intensities and could only be used with the $R = 0.99$ mirror set. The cuvette was then rotated to maximize the intensity reaching the detector and the rotation stage was locked. Coarse alignment of the cuvette in the vertical plane was checked by ensuring, using a spirit level, that the rotation stage was level with the optical table. There were no fine adjustments available for the vertical alignment. The front and back cavity mirrors were then further adjusted iteratively to maximize the output reaching the detector. The cuvette was subsequently filled and emptied with a syringe, ensuring minimum disturbance to the optimum alignment. The light exiting the cavity was focused by a 50 mm focal length lens onto the entrance of a 600 μm diameter, 1 m length, 0.22 numerical aperture quartz fiber (Thorlabs, UK). This was connected to the entrance slit of the spectrograph by an SMA905 fiber connection.

The experimental setup in principle allowed the measurement of the absorption spectrum of liquid- or solution-phase analytes at selected wavelengths in the range 400–700 nm depending on the output of the LED light source used. Many species are known to absorb in this region, so the choice of potential analytes was large. In general, most liquid-phase absorption spectra are broad (linewidths > 50 nm) and featureless. Exceptions to this include the solution-phase spectra of lanthanide ions, which have relatively sharp features (~ 5 nm linewidth) in their absorption spectrum. Holmium chloride, which produces Ho^{3+} ions in aqueous solution, was chosen as a species for study as some of the absorption features were coincident with the output of the red, green, and blue LEDs, and thus, this species could be studied at three separate wavelength regions. The use of a white LED with the $R = 0.99$ mirrors allowed the simultaneous measurement of all three absorption features. The other species chosen for study were the water-soluble food dye brilliant blue-R (Sigma Aldrich, UK), which has a broad absorption peaking at ~ 630 nm. The staining dye sudan black (Sigma Aldrich, UK), which had a broad absorption peaking at ~ 570 nm and which was soluble in nonpolar solvents such as hexane, and the fluorescent dye coumarin 334 (Sigma Aldrich, UK), which was soluble in polar solvents such as ethanol and had a broad absorption peaking at ~ 450 nm, were also chosen for study. All the dyes had large molar extinction coefficients (10^4 – 10^5 $\text{M}^{-1} \text{cm}^{-1}$), while that of Ho^{3+} was much smaller (~ 4 $\text{M}^{-1} \text{cm}^{-1}$). Preliminary measurements showed that the absorbance in the cavity had a linear dependence on the concentration of the analyte up to absorbance values of ~ 0.25 AU. Consequently, all measurements were made in the absorbance range of ~ 0.1 – 0.2 AU. This corresponded to concentrations of Ho^{3+} of $\sim 3 \times 10^{-3}$ M, brilliant blue-R of $\sim 1 \times 10^{-7}$ M, sudan black of $\sim 2.5 \times 10^{-6}$ M, and coumarin 334 of $\sim 2.5 \times 10^{-7}$ M.

The choice of solvents required some consideration as previous studies have noted problems with the use of hydrogen-bonded solvents such as water and methanol in the red part of the spectrum.²² This is due to the presence of background solvent absorption due to the fourth overtone of the O–H stretch at ~ 640 nm. Preliminary experiments were performed with brilliant blue-R dissolved in water and non-hydrogen-bonded polar solvents such as acetonitrile. For measurements in our 2 mm cell no difference could be

discerned in the maximum number of passes possible at around 640 nm. It should be noted that the previous study in which this issue was raised involved measurements in a 21 cm cell with higher reflectivity mirrors than those used in this study. Consequently, 18 $\text{M}\Omega\text{-cm}$ ultrapure water (Millipore) was used as the solvent for the Ho^{3+} and brilliant blue-R measurements. For the other analytes, spectrophotometric-grade solvents were used. Hexane (Fisher Scientific, UK) was used as the solvent for sudan black, while ethanol (Fisher Scientific, UK) was used as the solvent for coumarin 334.

Experimental Methodology. As noted earlier, one of the main disadvantages of CEAS based techniques is that unlike CRDS experiments, the absorption coefficient (α) cannot be directly calculated and instead must be obtained through a separate calibration. For the liquid-phase BBCEAS experiments reported in this study the calibration and the experimental methodology could be performed in a straightforward manner and were very similar to the experimental methodology for conventional UV-visible absorption spectroscopy. The calibration could be used to obtain in the first instance the cavity enhancement factor (CEF) or the number of passes made within the cavity. Once the effective path length had been calculated, the minimum detectable change in the absorption coefficient, α_{min} , could also be calculated. The first step in the calibration was to obtain a single-pass spectrum of the analyte to be studied. This could be performed in a standard 1 cm path length cuvette with a tungsten halogen light source and the same Avantes AVS2000 spectrometer. The concentration of the solution was typically a factor of ten higher than in the 2 mm cuvette in the cavity. An absorption spectrum was obtained by recording a background spectrum with just the solvent in the cuvette, I_0 , followed by the sample spectrum, I , and then the calculation of the absorbance from $ABS = \log_{10} I_0/I$. The Beer–Lambert law was then used to scale the peak of the absorption spectrum to the concentration used in the cavity and the 2 mm cuvette path length. This gave the single-pass absorbance under cavity conditions, ABS_{sp} . The cavity-enhanced absorption spectrum was obtained by first recording a background-solvent-only spectrum in the 2 mm cuvette. A sample spectrum was then recorded and the absorbance spectrum calculated. The value of the cavity-enhanced absorbance at the peak wavelength of the single-pass spectrum was measured. This gave the cavity absorbance, ABS_{cav} . The number of passes within the cavity or the CEF could be calculated as the ratio of ABS_{cav} to ABS_{sp} :

$$\text{CEF} = \frac{ABS_{\text{cav}}}{ABS_{\text{sp}}} \quad (2)$$

Given that the base path length was 2 mm, the effective path length of the measurement (l_{eff}) could also be calculated ($l_{\text{eff}} = \text{CEF} \times 0.2$ cm). Determination of the sensitivity of the measurement requires the calculation of α_{min} . For each measurement to obtain a CEF value, ten replicate measurements were also performed. The standard deviation in the absorbance value as a function of wavelength was calculated using a spreadsheet program (Microsoft Excel). The mean of the standard deviation values corresponded to the minimum detectable absorbance change ΔABS_{min} . The value of α_{min} could be obtained by dividing ΔABS_{min} by l_{eff} in cm. A factor of 2.303 is required to convert the absorbance values in \log_{10} units to \log_e units, which are the typical units of measurement for α_{min} . The calculated value of α_{min} is essentially the

TABLE I. A summary of the results obtained in terms of analyte, the LED used, the wavelength of measurement, the reflectivity of the mirrors, the CEF value, the minimum detectable change in absorption α_{\min} , the molar extinction coefficient ϵ at the wavelength of measurement, and the LOD of the analyte.

Analyte	LED	Wavelength (nm)	Reflectivity	CEF	α_{\min} (cm ⁻¹)	ϵ (M ⁻¹ cm ⁻¹)	LOD (M)
Ho ³⁺	Red	641	0.99	46 ± 0.2	6.7 × 10 ⁻⁵	3.35	2.6 × 10 ⁻⁵
Ho ³⁺	Red	641	0.9945	64 ± 1.1	3.9 × 10 ⁻⁴	3.35	1.5 × 10 ⁻⁴
Ho ³⁺	Red	641	0.999	104 ± 2.1	4.8 × 10 ⁻⁴	3.35	1.9 × 10 ⁻⁴
Ho ³⁺	Green	537	0.99	40 ± 0.2	1.6 × 10 ⁻⁴	4.67	4.4 × 10 ⁻⁵
Ho ³⁺	Green	537	0.9945	58 ± 1.2	6.4 × 10 ⁻⁴	4.67	1.8 × 10 ⁻⁴
Ho ³⁺	Blue	452	0.99	44 ± 0.5	1.8 × 10 ⁻⁴	3.61	6.3 × 10 ⁻⁵
Ho ³⁺	Blue	452	0.9945	65 ± 2.2	8.5 × 10 ⁻⁴	3.61	3.1 × 10 ⁻⁴
Ho ³⁺	White	641	0.99	47 ± 0.4	2.1 × 10 ⁻⁴	3.35	8.1 × 10 ⁻⁵
Ho ³⁺	White	537	0.99	40 ± 0.3	2.0 × 10 ⁻⁴	4.67	5.5 × 10 ⁻⁵
Ho ³⁺	White	452	0.99	44 ± 0.8	4.1 × 10 ⁻⁴	3.61	1.5 × 10 ⁻⁴
Brilliant blue-R	Red	630	0.99	51 ± 0.1	5.1 × 10 ⁻⁵	1.06 × 10 ⁵	6.2 × 10 ⁻¹⁰
Brilliant blue-R	Red	630	0.9945	60 ± 0.9	3.0 × 10 ⁻⁴	1.06 × 10 ⁵	3.7 × 10 ⁻⁹
Brilliant blue-R	Red	630	0.999	104 ± 3.1	6.0 × 10 ⁻⁴	1.06 × 10 ⁵	7.4 × 10 ⁻⁹
Sudan black	Red	620	0.99	59 ± 0.4	5.3 × 10 ⁻⁵	1.76 × 10 ³	3.9 × 10 ⁻⁸
Sudan black	Red	620	0.9945	74 ± 0.8	1.8 × 10 ⁻⁴	1.76 × 10 ³	1.3 × 10 ⁻⁷
Sudan black	Red	620	0.999	93 ± 2.7	3.9 × 10 ⁻⁴	1.76 × 10 ³	2.9 × 10 ⁻⁷
Sudan black	White	564	0.99	52 ± 0.3	1.9 × 10 ⁻⁴	4.72 × 10 ³	5.1 × 10 ⁻⁸
Coumarin 334	Blue	456	0.99	45 ± 0.5	2.0 × 10 ⁻⁴	5.07 × 10 ⁴	5.2 × 10 ⁻⁹
Coumarin 334	Blue	456	0.9945	53 ± 2.4	1.2 × 10 ⁻³	5.07 × 10 ⁴	3.1 × 10 ⁻⁸

minimum detectable change in the absorption coefficient:

$$\Delta\alpha_{\min} = \frac{2.303\Delta ABS_{\min}}{l_{\text{eff}}} \quad (3)$$

The limit of detection (LOD) of an analyte is usually calculated from the 99%, three standard deviations (3σ), confidence limit of the noise on the baseline of an absorption spectrum and thus could be calculated by dividing $3\alpha_{\min}$ by 2.303ϵ , where ϵ is the value of the molar extinction coefficient for the analyte under study at the wavelength of measurement. The ϵ values were experimentally determined using conventional UV-visible spectroscopy in a 1 cm cuvette, from plots of absorbance versus concentration data for the analytes at the wavelength of measurement. The mean values obtained from ten replicate measurements are listed in Table I, along with the wavelength of measurement.

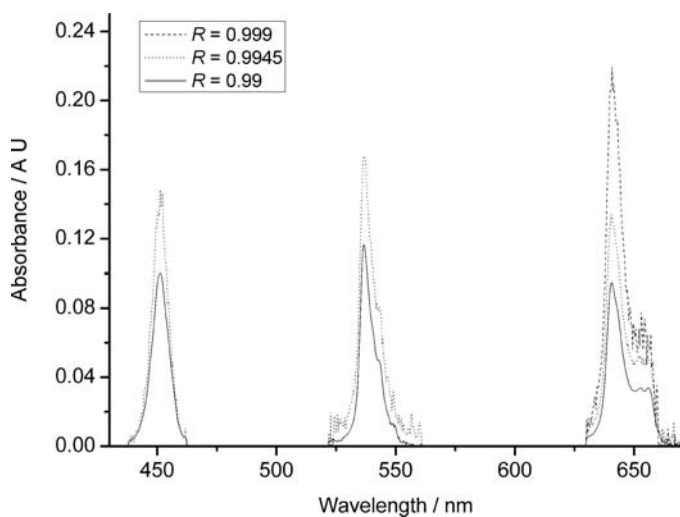


FIG. 2. The BBCEAS spectra of 3.1×10^{-3} M Ho³⁺ in water obtained using the red, green, and blue LEDs and the $R = 0.99$, 0.9945, and 0.999 mirror sets for the red LED and the $R = 0.99$ and 0.9945 mirror sets for the green and blue LEDs.

RESULTS

Liquid-phase BBCEAS measurements have been made in a 2 mm cuvette for four different analytes usually at the peak absorption wavelength, using appropriate LEDs and high reflectivity mirror sets. Table I summarizes the measurements made in terms of the analyte studied, the LED used, the wavelength of measurement, the reflectivity of the mirror set used, the CEF or number of passes obtained for each analyte (the 1σ error limit on the measurement is also shown), the calculated α_{\min} values for each measurement, the molar extinction coefficient ϵ of the analyte at the wavelength of measurement, and an estimation of the LOD for each analyte. Figure 2 shows representative absorption spectra of Ho³⁺ recorded with the $R = 0.99$ and 0.9945 mirror sets for the green and blue LEDs and the $R = 0.99$, 0.9945, and 0.999 mirror sets for the red LED. Figure 3 shows representative absorption spectra of brilliant blue-R recorded with the red LED and the R

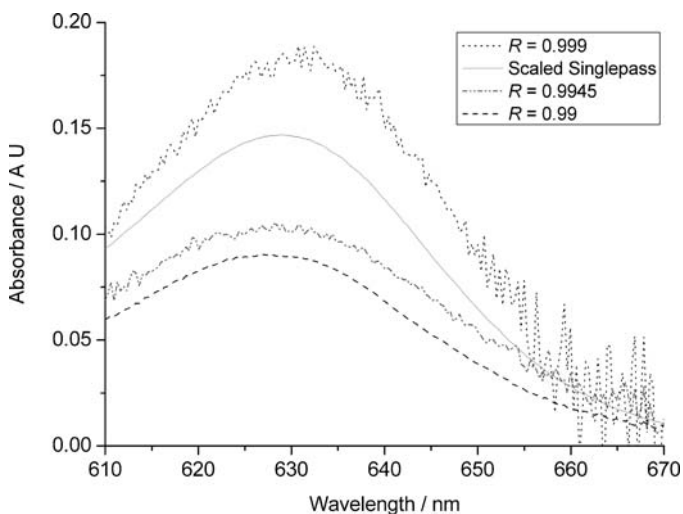


FIG. 3. The BBCEAS spectra of 7.9×10^{-8} M brilliant blue-R in water obtained using the red LED and the $R = 0.99$, 0.9945, and 0.999 mirror sets. A scaled single-pass spectrum is also shown.

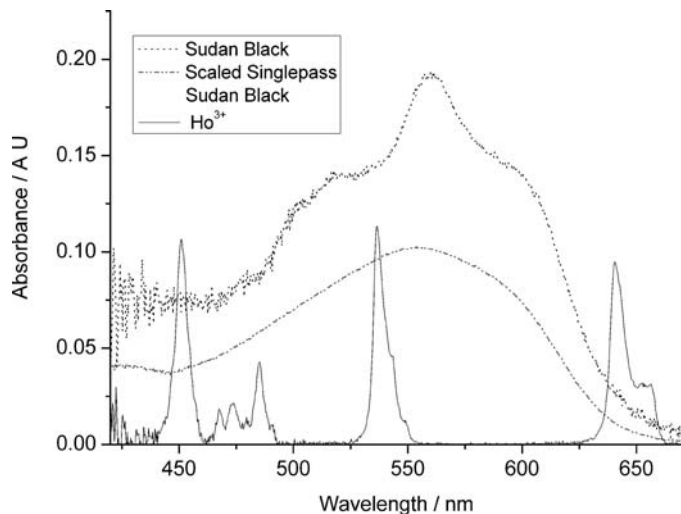


FIG. 4. The BBCEAS spectrum of 4.0×10^{-6} M sudan black in hexane and 3.1×10^{-3} M Ho^{3+} in water, in the range 420–670 nm, obtained with the white LED and the $R = 0.99$ mirror set. A scaled single-pass spectrum of sudan black is also shown.

= 0.99, 0.9945, and 0.999 mirror sets. Figure 4 shows representative absorption spectra recorded over a ~ 250 nm wavelength range in a single measurement for Ho^{3+} and sudan black using the white LED and the $R = 0.99$ mirror set.

Measurement of the Dynamic Range of the Technique.

To investigate the suitability of liquid-phase BBCEAS as an analytical tool, measurements were made on a selected analyte over a range of concentrations to determine the dynamic range of the technique and also provide an independent measurement of the LOD of the selected analyte. The analyte chosen was the dye brilliant blue-R, which was studied with the red LED and the $R = 0.99$ mirror set, as previous measurements with this combination of LED and mirror set yielded the lowest α_{\min} value and LOD. Figure 5 shows spectra of brilliant blue-R at a range of low concentrations from ~ 7 nM to ~ 50 nM. Figure 6 shows plots of absorbance versus concentration for brilliant blue-R. The brilliant blue-R measurements were made at 630

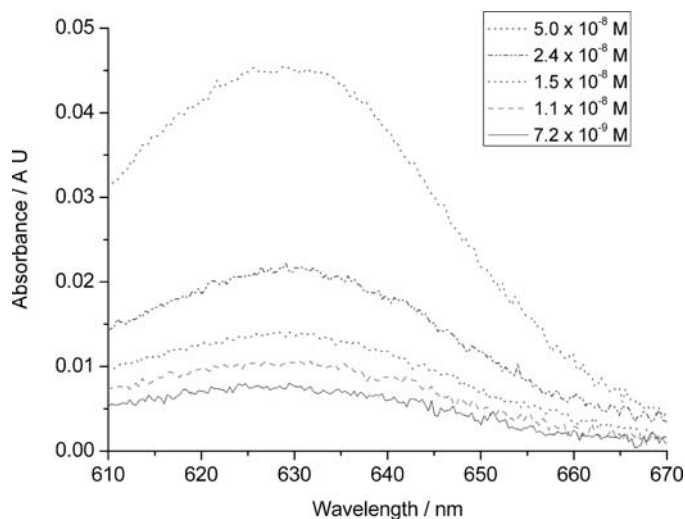


FIG. 5. BBCEAS spectra of brilliant blue-R, for a range of low concentrations from ~ 7 nM to ~ 50 nM, obtained using the red LED and the $R = 0.99$ mirror set.

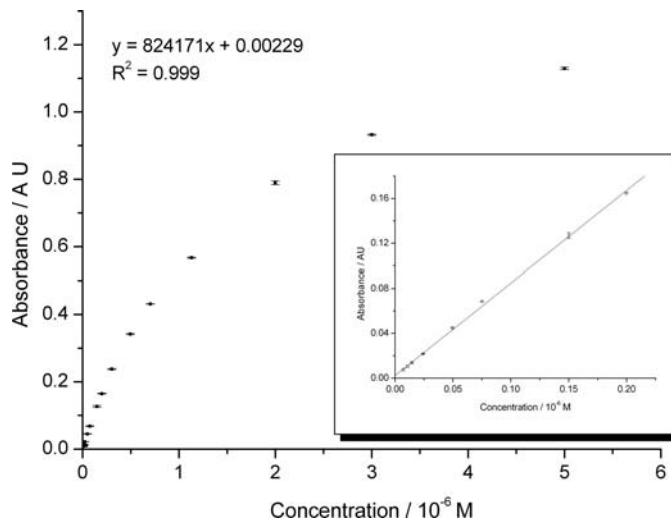


FIG. 6. An absorbance versus concentration plot of brilliant blue-R, in the range ~ 7 nM to ~ 5 μM , obtained using the red LED and the $R = 0.99$ mirror set. The inset shows the measurements in the linear range from ~ 7 nM to ~ 200 nM. The error bars represent the 1σ error limit of three replicate measurements at each concentration. The equation on the diagram refers to an error-weighted linear fit to the measurements shown in the inset.

nm and a range of concentrations from ~ 7 nM to ~ 5 μM . Three replicate measurements were made at each concentration and the error bars for each concentration represent the standard deviation of the measurements. The plot can be broken into two parts. The inset in Fig. 6 shows measurements in the range ~ 7 nM to ~ 200 nM, which show a linear dependence of the absorbance on the concentration. The measurements at higher concentrations, up to ~ 5 μM are nonlinear. An error-weighted regression through the linear part of the plot yields a straight line (equation of the line is given in Fig. 6) with $R^2 = 0.999$ and a 1σ error limit for the intercept of 3×10^{-4} . The LOD can be calculated from the value of the 3σ error limit on the intercept, which produces a concentration of 1.1 nM. This value is similar to the 620 pM LOD that was obtained from previous measurements with the red LED and the $R = 0.99$ mirror set, using the standard deviation of the noise on the absorbance measurement to determine the LOD. The limit of quantitation (LOQ) can also be determined from the 10σ error limit on the intercept and yields a concentration of 3.6 nM. At absorbance values above ~ 0.25 the plot in Fig. 6 is no longer linear with respect to increasing concentration, but measurements of absorbance values of up to ~ 1.2 were made without significantly visible increases in the 1σ error limit on three replicate measurements.

DISCUSSION

For each analyte, results have been obtained for values of the CEF, the α_{\min} , and also the LOD. These values are discussed in turn. The CEF values show the expected general trend of increasing for each analyte as the reflectivity of the cavity mirrors increases. The values of the CEF are, however, lower than would be expected in comparison with gas-phase measurements, for which in the limit of very high mirror reflectivity ($R \rightarrow 1$) and low absorption ($\alpha \rightarrow 0$) it can be shown that¹⁴

$$\frac{I_0}{I} = 1 + \frac{\alpha l}{1 - R} \quad (4)$$

TABLE II. A comparison between this study and previous liquid-phase cavity studies as a function of technique, the mirror reflectivity, base path length, the wavelength of measurement, the lowest value of α_{\min} , the minimum LOD for an analyte, and the molar extinction coefficient ϵ for that analyte.

Study	Technique	Mirror reflectivity	Base path length (cm)	Wavelength (nm)	α_{\min} (cm ⁻¹)	LOD (M)	ϵ (M ⁻¹ cm ⁻¹)
This work	BBCEAS	0.99	0.2	630	5.1×10^{-5}	6.2×10^{-10}	1.06×10^5
Xu et al. ¹⁹	CRDS	0.9997	1	607	1×10^{-5}
Snyder et al. ²⁰	CRDS	0.9993	0.03	470	2.5×10^{-4}	9.2×10^{-8}	9×10^3
Hallock et al. ²²	CRDS	0.9998	21	620–670	1×10^{-6}	$\sim 1 \times 10^{-11}$	1×10^5
Hallock et al. ²³	CRDS	0.9998	23	655	3.3×10^{-7}
Bechtel et al. ²⁴	CRDS	...	0.03	488	2.6×10^{-6}	1×10^{-7}	...
Bahnev et al. ²⁵	CRDS	0.9998	0.2	532	1.6×10^{-4}	3.7×10^{-9}	5.45×10^4
van der Sneppen et al. ²⁶	CRDS	0.99996	0.2	532	1.0×10^{-5}	1.5×10^{-8}	1.4×10^4
van der Sneppen et al. ²⁷	CRDS	0.99993	0.2	457	1.0×10^{-5}	1.2×10^{-8}	3.6×10^4
van der Sneppen et al. ²⁷	CRDS	0.9995	0.2	355	5.0×10^{-5}	7.5×10^{-8}	1.02×10^4
Fiedler et al. ²⁸	BBCEAS	0.99	1	607	2×10^{-5}
Fiedler et al. ²⁸	BBCEAS	0.99	0.1	607	3×10^{-5}
McGarvey et al. ²⁹	CEAS	0.99998	0.175	783	7×10^{-6}	2×10^{-10}	6×10^4
Alexander ³⁰	CRDS	0.9998	2.32×10^{-3}	628	5.4×10^{-3}	7.1×10^{-8}	1×10^5

A conventional single-pass experiment can be expressed as $I_0/I = 1 + \alpha l$, that is, the increase in the number of passes and sensitivity for a cavity-based experiment is given by $(1 - R)^{-1}$. This assumes that absorption and scattering losses by the mirrors are low and that scattering losses by the gas-phase sample are insignificant and the absorption is small. For most gas-phase measurements all these conditions are satisfied. For the liquid-phase measurements in this study there are additional losses due to scattering and absorption by the solvent as well as the cuvette windows. These losses could be measured for the system in this study by recording the intensity of light exiting the cavity in the absence and presence of the cuvette and solvent and from the knowledge of the number of passes for a given mirror set. Measurements with the $R = 0.99$ mirror set showed that the combined cuvette and solvent losses were $\sim 1 \times 10^{-2}$ per pass, which is consistent with the lower than expected increase of the CEF values with increasing mirror reflectivity. This value is, however, rather high compared with the only other liquid-phase BBCEAS study, of Fielder et al.²⁸ They reported cuvette losses of $\sim 10^{-3}$ per pass and solvent losses of $\sim 10^{-3}$ cm⁻¹. Single-pass measurements on the solvents in a 1 cm cuvette indicated losses of $\sim 10^{-3}$ cm⁻¹ across the 450 to 650 nm range and so suggest that the solvents are unlikely to be responsible for the higher than expected loss. Possible explanations for the higher than expected loss include the lack of fine adjustment for the vertical alignment of the cuvette in the cavity, lack of coplanarity of the cuvette windows, and less than optimal polishing of cuvette windows, leading to increased scattering from the optical surfaces.

One advantage of BBCEAS experiments is that measurements can be made over a wide wavelength range usually limited by the bandwidth of the cavity mirrors used or the bandwidth of the light source. The measurements on Ho³⁺ and sudan black with the white LED and the $R = 0.99$ mirrors spanned a wavelength range of ~ 250 nm and represent the largest wavelength range covered to date in a single BBCEAS experiment. As demonstrated by the Ho³⁺ measurements, coverage of a broad wavelength range allows in principle several transitions to be measured in a single experiment.

The separate measurement of the Ho³⁺ transitions with the white LED as well as the red, green, and blue LEDs and the $R = 0.99$ mirror set allows the reproducibility and robustness of the technique to be assessed. The independent CEF values for the red, green, and blue transitions obtained using the two separate light sources are almost identical within the error

limits of the measurement, thus indicating that the CEF values are highly reproducible. The variation in the CEF values between the red, green, and blue transitions is most likely due to variations in the reflectivity profile of the $R = 0.99$ mirror set as a function of wavelength. For the other analytes, the CEF values show the general trend of increasing with mirror reflectivity. For a given mirror reflectivity the differences in values between the analytes are again most likely due to variations in the reflectivity profile of the mirror sets. The ripples in the reflectivity versus wavelength profile were most significant for the $R = 0.99$ mirror set due to the nature of their design. The ripples occur over ~ 50 nm and for narrow linewidth spectra such as Ho³⁺ result in no visible distortion of the shape of the spectral features. Even for moderately broad absorptions such as that of brilliant blue-R in Fig. 3 the spectral distortion, at least visually, is marginal. For broad absorptions such as that of sudan black in Fig. 4, the spectral distortion is more significant. The single-pass spectrum of sudan black is by comparison broad and featureless. The spectral distortion could be corrected by knowledge of the form of the reflectivity profile either from the manufacturer's data sheet or from independent CRDS measurements. A simpler procedure could be to obtain the form of the reflectivity profile by taking the ratio of the BBCEAS spectrum of a broad absorber to the single-pass spectrum and using that data to correct all other spectra.

The sensitivity of most cavity-based experiments is determined from the minimum detectable change in the absorption coefficient, α_{\min} . This typically refers to the standard deviation of the noise on the baseline of the measurement. From Table I it can be seen that the values obtained in this study range from 5.1×10^{-5} cm⁻¹ to 1.2×10^{-3} cm⁻¹. Standard gas-phase cavity measurements typically report α_{\min} values of $< 10^{-7}$ cm⁻¹.¹⁴ In comparison, the values from this study are significantly higher; however, this is not surprising because the α_{\min} values are inversely proportional to the total path length and so are affected by both the short base path length of 2 mm and also the relatively low number of passes. In gas-phase studies a base path length of ~ 1 m and more than a 1000 passes through the sample are common. It is consequently more appropriate to make comparisons with other liquid-phase cavity-based studies.

Comparison with Previous Liquid-Phase Cavity Studies. Table II summarizes some of the figures of merit obtained from this study such as the lowest value of α_{\min} obtained, the lowest LOD obtained, and the molar absorption coefficient for the

analyte in question. These are compared with corresponding data, where available, from the small number of previous liquid-phase cavity studies. Table II also lists the base path length of the measurement, the wavelength of measurement, and the reflectivity of the cavity mirrors used in the studies. A discussion of the α_{\min} values and the LOD values is undertaken in the paragraphs below.

The CRDS studies related to HPLC detection have typically quoted the baseline noise in absorbance units (AU), but these can be converted to α_{\min} values by multiplying by 2.303 to convert from \log_{10} units to \log_e units and then dividing by the path length of the cell in cm. Care must be taken that the comparison is made with the root mean squared (rms) 1σ noise value rather than the peak-to-peak 3σ noise value, which is often stated. For example, van der Sneppen et al.²⁶ reported the baseline noise in their study to be 2.7×10^{-6} AU, peak to peak, in a 2 mm path length cell. This corresponds to an rms value of $\sim 9 \times 10^{-7}$ AU, which produces an α_{\min} value of 1.0×10^{-5} cm^{-1} .

Comparing with the results from this study, it can be seen that the mirror reflectivities used in the previous liquid-phase studies are generally much higher. The lowest α_{\min} value obtained in this study, 5.1×10^{-5} cm^{-1} , was obtained using $R = 0.99$ mirrors. The base path length of 2 mm is in the middle of the range of those used in the previous studies. The values of α_{\min} obtained consequently compare surprisingly favorably with the previous studies given the simplicity of the experimental setup and the data analysis. The study carried out by Fiedler et al.²⁸ is the most similar to the current one. Their measurements using a modified double-beam UV-visible spectrometer and a 1 cm cell, with $R = 0.99$ mirrors, yielded similar values of α_{\min} of $\sim 2 \times 10^{-5}$ cm^{-1} , albeit with a five times longer base path length and a double beam setup. Separate measurements in a 1 mm cell using a high intensity Xe arc lamp as the light source and a CCD spectrograph detector produced an α_{\min} of $\sim 3 \times 10^{-5}$ cm^{-1} , which is similar to our values but using a significantly more expensive light source.

The values of α_{\min} in Table I are generally seen to increase as the reflectivity of the mirrors increases. This counterintuitive trend is attributable to the decrease in the intensity of light reaching the detector as the reflectivity of the mirrors increases. This required the integration time on the CCD array to be increased to enhance the signal, but due to the lack of thermoelectric cooling of the CCD array, integration times longer than ~ 100 ms resulted in nonlinear increases in the dark noise. This manifested itself in increased noise on the absorbance measurement and consequently higher values of α_{\min} . Aside from the $R = 0.99$ mirror sets, all the other mirror sets required the use of integration times in excess of 100 ms. Thus, even though the effective path length increased with the use of higher reflectivity mirror sets, the increase in noise due to increased dark noise from longer integration times usually resulted in poorer values of α_{\min} .

Table I also lists the LOD values for the analytes studied based on the calculated value of α_{\min} and ϵ of the analyte. For the strong absorber brilliant blue-R ($\epsilon \sim 1 \times 10^5$ $\text{M}^{-1} \text{cm}^{-1}$ at 630 nm), it has been shown that the minimum LOD is approximately 620 pM. The value of the LOD of an analyte will depend on both ϵ and the path length of the measurement. In general, longer path lengths and larger values of ϵ will produce lower LODs. The most appropriate comparison is with

the CEAS study carried out by McGarvey et al.,²⁹ which reported an LOD for bacteriochlorophyll *a* ($\epsilon \sim 6 \times 10^4$ $\text{M}^{-1} \text{cm}^{-1}$ at 783 nm) of approximately 200 pM using much higher reflectivity $R = 0.99998$ mirrors and a significantly more complex and expensive experimental setup. Comparisons of the LOD values obtained in this study can also be made with the previous studies related to CRDS measurements on HPLC systems, as these typically report LOD measurements on strong absorbers such as dye molecules. It should be noted that in general the HPLC studies report LODs based on the injected concentration before LC separation. Chromatographic broadening results in the concentration in the detection cell being significantly lower.

Taking into account differences in the base path length, as well as the molar extinction coefficients of the analytes studied, the LOD values from this study compare very favorably with the previous studies, especially given the simplicity of the experimental setup and the data analysis. Indeed, BBCEAS would appear to offer some advantages over CRDS as a method of detection for HPLC systems. Short base path lengths do not increase the experimental difficulty, whereas previous CRDS studies have either required picosecond lasers and nanosecond timescale detection for HPLC cells where the mirrors are in contact with the liquid²⁵⁻²⁷ or a large separation between the cavity mirrors to produce measurable ring-down times for slower detection schemes.^{20,21,24} The dynamic range of CRDS measurements is restricted at higher concentrations by the ring-down time approaching the measurement limit of the detection system. For BBCEAS measurements, a linear dynamic range of measurement of about two orders of magnitude, from the LOD of $\sim 1 \times 10^{-3}$ AU to 0.2 AU, has been shown. For larger absorbance values, up to the maximum measured value of 1.2, where the response becomes nonlinear, the concentration can in principle still be quantified using a calibration curve. The nonlinear behavior at higher concentrations is attributed to the increasing absorbance due to the analyte, resulting in a reduction in the number of passes in the cavity and consequently a reduction in the effective path length. The multiplex nature of detection used in BBCEAS also offers the advantage of detecting simultaneously over a range of wavelengths and thus does not require the analytes to all absorb at a single wavelength. It is in fact analogous to modern HPLC systems, which typically use multichannel diode array detectors for UV-visible detection rather than a single wavelength detector.

The sensitivity of the experimental setup could be improved in a number of ways. The simplest improvement would be to increase the path length of the cuvette. Most conventional implementations of liquid-phase UV-visible spectroscopy tend to use 1 cm cuvettes, and this would in principle decrease the α_{\min} values by a factor of five without increasing the experimental difficulty or the applicability of the technique. It has been shown that the use of $R = 0.999$ mirrors increases the effective path length by a factor of approximately 2.5 compared to $R = 0.99$ mirrors, but there is not a corresponding improvement in the sensitivity due to increased noise from the uncooled CCD detector at longer integration times. This could be addressed by using either a cooled detector, which would allow the use of longer integration times without the associated increase in dark noise, or a higher intensity light source, which would allow shorter integration times to be used.

Given that at best only about 1% of the output of the LED could be effectively used, a more efficient method of coupling the LED output into the cavity would also allow the use of shorter integration times for the higher reflectivity mirrors. These changes would in principle improve the sensitivity of the technique such that an α_{\min} of $\sim 2 \times 10^{-6} \text{ cm}^{-1}$ could be achieved, allowing the detection of strong absorbers ($\epsilon \sim 1 \times 10^5 \text{ M}^{-1} \text{ cm}^{-1}$) down to the 50 pM level. Further improvements could be made by reducing the reflection and scattering losses in the cavity, which would lead to greater effective path lengths with the higher reflectivity mirrors. This could be achieved by better fine control of the vertical alignment of the cuvette in the cavity, polishing the cuvette windows, and also ensuring that the cuvette windows are as parallel as possible during manufacture. Alternatively, the use of a cavity without a cuvette, where the mirrors are in direct contact with the analyte, would also reduce scattering and absorption losses.

The BBCEAS technique has the potential to become a widely applicable analytical technique for the study of liquid-phase species and complement existing applications of UV-visible spectroscopy for which more sensitive detection is needed. Indeed, Fielder et al.²⁸ have already demonstrated that it is possible to convert a conventional scanning monochromator UV-visible spectrometer to operate as a BBCEAS spectrometer in the 450 to 650 nm range. The general requirements for a BBCEAS spectrometer to function across the UV-visible wavelength range are suitable light sources, mirrors, and detectors. CCD spectrographs that operate over the entire spectral range of traditional UV-visible spectroscopy (200–700 nm) are commonplace. Likewise, broadband lamps such as Xe arc lamps also output over most of the UV-visible wavelength range. Cheaper high intensity light sources such as tungsten-halogen lamps output only over the visible part of the spectrum, while LEDs are commonly available over visible wavelengths and are starting to become available at selected wavelengths in the UV down to wavelengths as short as 240 nm. Ideally, BBCEAS in the UV-visible region would be performed with one large bandwidth mirror set covering the range 200–700 nm with $R > 0.99$ and a relatively flat reflectivity versus wavelength profile. This, however, is not possible at the moment. Currently, suitable mirrors with a 300 nm bandwidth covering the entire visible range (400–700 nm) with $R > 0.995$ are available as custom designs, but producing suitable broad bandwidth mirrors in the UV range remains a far more difficult challenge. Nevertheless the components already exist to produce a simple low-cost BBCEAS spectrometer that would operate across most of the UV-visible spectrum as either a stand-alone instrument or as an add-on to a conventional UV-visible spectrometer.

CONCLUSION

A simple low-cost BBCEAS experimental setup has been demonstrated for the measurement of four representative liquid-phase analytes in a 2 mm quartz cuvette at a range of wavelengths in the visible part of the electromagnetic spectrum and using mirror sets with three different reflectivities. The methodology for the measurement of the absorption spectrum requires a simple calibration and is conceptually similar to standard UV-visible absorption spectroscopy. The results yielded the number of passes through the sample or the CEF, as well as the sensitivity of the measurement through the

minimum detectable change in absorbance, α_{\min} . The limit of detection for each analyte was also calculated. The use of a white LED and $R = 0.99$ mirrors allowed measurements in the range $\sim 420\text{--}670 \text{ nm}$ to be made in a single experiment. The CEF values were found to generally increase with higher mirror reflectivities, although the increase was significantly less than expected in comparison with gas-phase measurements. This was attributed to relatively large scattering and absorption losses from the cuvette windows. The α_{\min} values tended to increase with increasing mirror reflectivities due to lower levels of light reaching the detector and, consequently, increasing amounts of dark noise from the detector at the longer integration times needed to make the measurements. Consequently, for the current experimental setup the most sensitive measurements were made with the lowest reflectivity $R = 0.99$ mirror set. In comparison with previous cavity based studies on liquids, the lowest α_{\min} values from this study were found to offer similar levels of sensitivities to the best previous measurements, using in general much lower reflectivity mirrors and a simpler experimental setup and data analysis. Likewise, the limits of detection for strong absorbers were comparable to the best results obtained from previous CRDS studies on HPLC systems and suggest that BBCEAS might provide a sensitive but simple method of detection for HPLC systems. Finally, some suggestions to improve the sensitivity of the experimental setup were made and some technical challenges that need to be overcome to make BBCEAS a widely applicable analytical technique were identified.

ACKNOWLEDGMENTS

The authors would like to thank the University of Teesside, University Research Fund, for financial support. The authors are grateful to Professor Gus Hancock, Dr. Grant Ritchie, Dr. Rob Peverall, and Dr. Wolfgang Denzer (The PTCL, University of Oxford) for advice and loan of cavity mirrors and optical components. M.I. would like to acknowledge financial support from the EPSRC Portfolio grant *LASER* through which he was able to visit Professor Hancock's group in Oxford.

1. A. O'Keefe and D. A. G. Deacon, *Rev. Sci. Instrum.* **59**, 2544 (1988).
2. R. Engeln, G. Berden, R. Peeters, and G. Meijer, *Rev. Sci. Instrum.* **69**, 3763 (1998).
3. A. O'Keefe, *Chem. Phys. Lett.* **293**, 331 (1998).
4. R. Peeters, G. Berden, A. Olafsson, L. J. J. Laafhoven, and G. Meijer, *Chem. Phys. Lett.* **337**, 231 (2001).
5. S. E. Fiedler, A. Hese, and A. A. Ruth, *Chem. Phys. Lett.* **371**, 284 (2003).
6. S. M. Ball, J. M. Langridge, and R. L. Jones, *Chem. Phys. Lett.* **398**, 68 (2004).
7. J. M. Langridge, S. M. Ball, and R. L. Jones, *Analyst (Cambridge, U.K.)* **131**, 916 (2006).
8. M. D. Wheeler, S. M. Newman, A. J. Orr-Ewing, and M. N. R. Ashfold, *J. Chem. Soc. Faraday Trans.* **94**, 337 (1998).
9. K. W. Busch and M. A. Busch, Eds., *Cavity-Ringdown Spectroscopy* (American Chemical Society, Washington, D.C., 1999).
10. G. Berden, R. Peeters, and G. Meijer, *Int. Rev. Phys. Chem.* **19**, 565 (2000).
11. D. B. Atkinson, *Analyst (Cambridge, U.K.)* **128**, 117 (2003).
12. S. S. Brown, *Chem. Rev.* **103**, 5219 (2003).
13. S. M. Ball and R. L. Jones, *Chem. Rev.* **103**, 5239 (2003).
14. M. Mazurenka, A. J. Orr-Ewing, R. Peverall, and G. A. D. Ritchie, *Annu. Rep. Prog. Chem., Sect. C* **101**, 100 (2005).
15. N. J. Van Leeuwen, H. G. Kjaergaard, D. L. Howard, and A. C. Wilson, *J. Mol. Spectrosc.* **228**, 83 (2004).
16. D. Romanini, M. Chenevier, S. Kassi, M. Schmidt, C. Valant, M. Ramonet, J. Lopez, and H.-J. Jost, *Appl. Phys. B* **83**, 659 (2006).
17. R. S. Brown, I. Kozin, Z. Tong, R. D. Oleschuk, and H.-P. Looock, *J. Chem. Phys.* **117**, 10444 (2002).
18. H.-P. Looock, *Trends Anal. Chem.* **25**, 655 (2006).
19. S. Xu, G. Sha, and J. Xie, *Rev. Sci. Instrum.* **73**, 255 (2002).
20. K. L. Snyder and R. N. Zare, *Anal. Chem.* **75**, 3086 (2003).

21. A. J. Alexander, *Chem. Phys. Lett.* **393**, 138 (2004).
22. A. J. Hallock, E. S. F. Berman, and R. N. Zare, *Anal. Chem.* **74**, 1741 (2002).
23. A. J. Hallock, E. S. F. Berman, and R. N. Zare, *Appl. Spectrosc.* **57**, 571 (2003).
24. K. L. Bechtel, R. N. Zare, A. A. Kachanov, S. S. Sanders, and B. A. Paldus, *Anal. Chem.* **77**, 1177 (2005).
25. B. Bahnev, L. van der Sneppen, A. E. Wiskerke, F. Ariese, C. Gooijer, and W. Ubachs, *Anal. Chem.* **77**, 1188 (2005).
26. L. van der Sneppen, A. Wiskerke, F. Ariese, C. Gooijer, and W. Ubachs, *Anal. Chim. Acta* **558**, 2 (2006).
27. L. van der Sneppen, A. Wiskerke, F. Ariese, C. Gooijer, and W. Ubachs, *Appl. Spectrosc.* **60**, 931 (2006).
28. S. E. Fiedler, A. Hese, and A. A. Ruth, *Rev. Sci. Instrum.* **76**, 023107-1 (2005).
29. T. McGarvey, A. Conjusteau, and H. Mabuchi, *Opt. Express* **14**, 10441 (2006).
30. A. J. Alexander, *Anal. Chem.* **78**, 5597 (2006).